

# Real-Time Synchronized Interaction Framework for Emotion-Aware Humanoid Robots\*

Yanrong Chen<sup>1</sup> and Xihan Bian<sup>2</sup>

**Abstract**—As humanoid robots increasingly introduced into social scene, achieving emotionally synchronized multimodal interaction remains a significant challenges. To facilitate the further adoption and integration of humanoid robots into service roles, we present a real-time framework for NAO robots that synchronizes speech prosody with full-body gestures through three key innovations: (1) A dual-channel emotion engine where large language model (LLM) simultaneously generates context-aware text responses and biomechanically feasible motion descriptors, constrained by a structured joint movement library; (2) Duration-aware dynamic time warping for precise temporal alignment of speech output and kinematic motion keyframes; (3) Closed-loop feasibility verification ensuring gestures adhere to NAO’s physical joint limits through real-time adaptation. Evaluations show 21% higher emotional alignment compared to rule-based systems, achieved by coordinating vocal pitch (arousal-driven) with upper-limb kinematics while maintaining lower-body stability. By enabling seamless sensorimotor coordination, this framework advances the deployment of context-aware social robots in dynamic applications such as personalized healthcare, interactive education, and responsive customer service platforms.

## I. INTRODUCTION

As robotic systems increasingly permeate social domains including healthcare, education, and service industries, the demand for emotionally resonant and temporally coordinated human-robot interaction (HRI) has become critical. Studies show that gesture-speech synchronization can significantly enhance users’ perception of empathy and engagement [1]. Despite this, achieving real-time co-speech gesture generation in physically embodied systems remains an open challenge, constrained by three core factors: (1) the high-dimensional complexity of motion dynamics [2], (2) variability in speech prosody and affective shifts [3], and (3) strict biomechanical constraints of robotic platforms such as NAO [4].

Early gesture synthesis systems primarily relied on rule-based mappings between predefined linguistic cues and gesture templates [5], which were limited in adaptability. Data-driven approaches later introduced statistical learning from curated datasets [6], enabling more flexible outputs but often remained constrained to 2D gestures or static mappings. The advent of deep generative models, such as Human Motion

\*This work was supported by Xi'an Jiaotong-Liverpool University under internal research funding. The NAO humanoid robot was provided by the university. The large language model resources were supported by Alibaba Cloud. Project guidance was provided by Dr. Xihan Bian. Project Website: <https://cyr1213.github.io/ReSIn-HR/>

<sup>1</sup>Yanrong Chen is with the Department of Computing, Xi'an Jiaotong-Liverpool University, Suzhou, China. chenyanrong2025@163.com

<sup>2</sup>Xihan Bian is with the Department of Computing, Xi'an Jiaotong-Liverpool University, Suzhou, China. xihan.bian@xjtlu.edu.cn

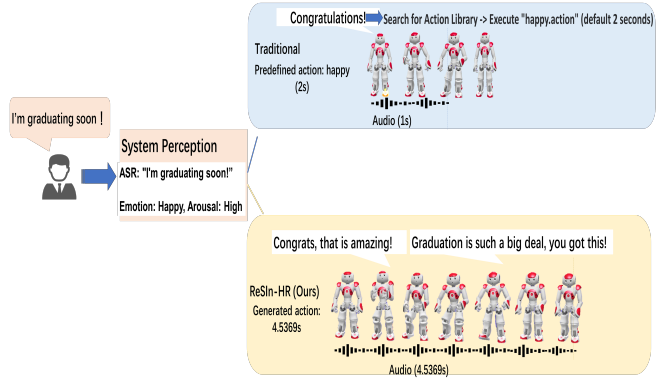


Fig. 1: Traditional gesture systems play static actions disconnected from speech timing. ReSIn-HR generates dynamic, emotionally aligned gestures that synchronize with both content and prosody.

Diffusion Models (HMDMs) [7], [8], allowed for temporally coherent and stylistically consistent full-body motion synthesis. Techniques like DiffSHEG [9] and MoFusion [8] leveraged affect-conditioned diffusion or transformer-based pipelines to produce expressive gesture sequences, yet they often rely on pre-segmented emotion labels and are not optimized for real-time interaction.

Recent developments in using large language models (LLMs) for embodied control [10], [11] have demonstrated that linguistic input can be mapped directly to low-level control actions. Building on this foundation, works such as MotionGPT [12] explore LLMs for high-level motion synthesis. However, these frameworks typically focus on semantic alignment and omit real-time emotional adaptation or physical constraint integration. To address these challenges, this work introduces **ReSIn-HR** (Real-time Synchronized Interaction for Humanoid Robots), a novel framework for synchronized speech-gesture generation. Our approach integrates real-time speech emotion recognition (SER) with adaptive gesture planning, offering the following three core innovations:

### 1) Dual-Stream Emotion Processing

A pipeline that extracts both linguistic and prosodic cues to inform gesture selection, enabling emotion-driven motion adaptation.

### 2) Duration-Aware Synchronization

A mechanism that dynamically predicts speech duration and adjusts gesture keyframes to minimize timing misalignment.

### 3) Biomechanical Constraint Verification

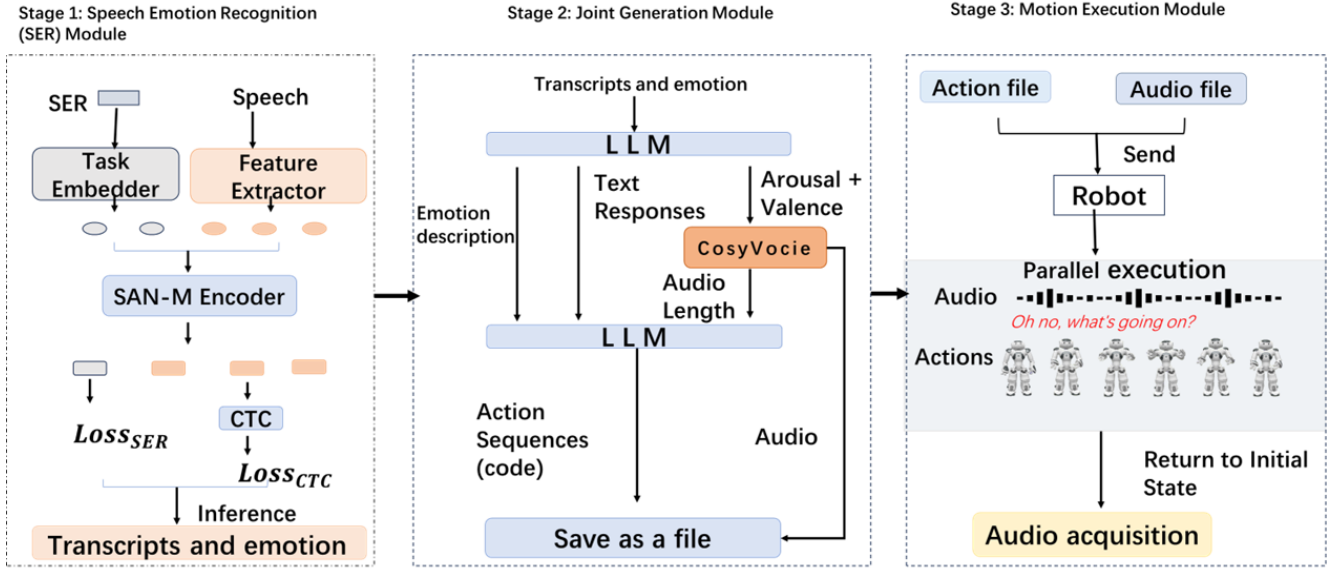


Fig. 2: System architecture of ReSIn-HR for multimodal interaction.

A real-time module that ensures generated gestures adhere to the robot’s physical limitations, preventing unnatural movements or execution failures.

**Experimental validation** with the NAO robot demonstrates that the ReSIn-HR framework achieves a **21% higher emotional alignment** compared to a rule-based NAO system. By unifying affective signal processing, temporal coordination, and hardware-aware motion synthesis, ReSIn-HR advances the state of the art in socially adaptive human-robot interaction (HRI), enabling robots to produce contextually appropriate gestures that align with both linguistic content and emotional tone in real time.

Fig 1 compares a rule-based system with our ReSIn-HR framework. While the traditional method plays a fixed “happy” gesture disconnected from speech dynamics, our system generates emotionally appropriate and temporally synchronized gestures that evolve naturally with the utterance. This demonstrates ReSIn-HR’s ability to deliver expressive, speech-aware motion, enhancing the fluidity and empathy of robot interaction.

## II. RELATED WORK

**Emotion-Aware Gesture Generation:** Early approaches to gesture synthesis relied on rule-based mappings [13], [14] and statistical models [15], [16], which suffered from limited generalizability due to handcrafted rules and small datasets. With the advent of 3D human pose estimation [17], [18] and deep temporal models [19], [20], data-driven methods emerged, learning gesture patterns from audio, text, and speaker identity. Emotion-conditioned models introduced valence-arousal modulation and affective GANs [21], but typically rely on scripted datasets and struggle in real-time, spontaneous interaction. In addition, gesture timing has been explored via prosodic cues [22] and latent alignment [23], though robustness remains an issue under hardware latency and spontaneous speech. Our work builds upon these foundations by integrating real-time emotion detection with gesture

generation, using speech duration and emotion shifts as soft anchors for synchronization.

**LLMs for Motion and Gesture Synthesis:** Recent progress in robot control has leveraged large language models (LLMs) to bridge language and action. Code-as-Policies [10] and RT-2 [11] show that LLMs can translate textual prompts into executable policies. MotionGPT [12] and MoFusion [8] extend this to text-to-motion generation by embedding prompts into continuous motion spaces. However, most models focus on semantic alignment, with limited emotional modulation. Emotion-aware gesture generation [5], [9] often depends on fixed emotion categories and external classifiers, while motion feasibility is treated as a post-processing step. Prompt engineering for robotic planning has introduced symbolic and programmatic structures, but lacks integration of dynamic features like affect curves or joint constraints. We extend this line by encoding multimodal constraints—including valence-arousal over time, semantic intent, and joint limits—directly into LLM prompts, enabling expressive and physically valid gesture generation.

**Comparison and Positioning:** While prior work has explored co-speech gesture generation from various modalities, limitations persist in real-time synchronization, emotional grounding, and robotic feasibility. Our framework unifies language, affect, and motion constraints into a single LLM query, enabling closed-loop gesture generation that is emotionally expressive, temporally aligned, and directly executable on the NAO platform. By integrating speech emotion recognition (SER), timing-aware gesture planning, and prompt-based motion synthesis, our approach advances the design of responsive, embodied dialogue systems for real-world HRI scenarios.

### III. METHODOLOGY

#### A. System Architecture

The proposed system adopts a three-tier hierarchical architecture designed to support emotion-coordinated multimodal interaction. As depicted in Fig. 2, this framework enables the NAO robot to respond naturally with dynamically synchronized speech, gestures, and emotional expressions in real time.

**Speech Emotion Recognition (SER) Module:** This multimodal speech analyzer employs SenseVoice to extract both linguistic and affective features from user speech. The extracted information includes valence and arousal values, which quantify the emotional intensity and polarity of the speech. Additionally, the module estimates the duration of the speech, which is essential for ensuring temporal alignment with generated gestures.

**Joint Generation Module:** We utilize the Qwen Large Language Model [12] to process the SER outputs and generate an emotionally congruent textual response with structural alignment. It also generates gesture descriptors aligned with the speech content and emotional state, using deep learning to dynamically adapt gestures to emotional and linguistic cues.

**Motion Execution Module:** Once the gestures are generated, A real-time motion planner translates gesture descriptors into executable motor commands tailored for the NAO robot. To minimize speech-gesture asynchrony, a dynamic timing controller adjusts key frames' durations based on the SER-predicted speech length. This will enhance interaction fluidity, minimizing perceptible delays or misalignments.

#### B. Emotion-Driven Gesture Generation

1) *LLM-Guided Motion Planning:* As outlined in Algorithm 1, the LLM-guided motion planning framework employs through a two-stage pipeline: (i) retrieving semantically relevant gesture examples from a motion library based on emotional queries, and (ii) prompting a large language model (LLM) to synthesize continuous, physically plausible motion sequences aligned with both emotion intent and utterance content.

Given an input utterance, the system first segments the sentence into discrete emotional phrases (e.g., *"I feel so sorry"*). Each phrase then serves as a semantic query to retrieve top- $k$  gesture examples from a predefined motion library, by utilizing a transformer-based sentence embedding model. These retrieved gestures provide stylistic and semantic priors for subsequent synthesis.

The generation prompt submitted to the LLM encodes five key elements: the emotional phrase and its corresponding text segment, semantically retrieved gesture examples from the motion library, physical constraints (e.g., joint limits and forbidden joints), stylistic guidelines (e.g., slowness, smoothness, medium amplitude), and transition constraints based on the final pose of the previous segment. By integrating these components, the LLM can generate expressive and physically valid motion segments in precise keyframe code format.

---

#### Algorithm 1 Emotion-Aware Gesture Generation via Prompt-Based LLM Planning

---

```

1: Input: Emotion segments  $\{(q_i, t_i)\}_{i=1}^n$ , Motion library
    $\mathcal{L}$ , Joint constraints  $\mathcal{C}$ 
2: Output: Executable gesture sequence  $\mathcal{G} = \{g_i\}_{i=1}^n$ 
3: for each segment  $(q_i, t_i)$  do
4:   Retrieve top- $k$  gesture examples:  $\{(K_j, V_j)\}_{j=1}^k \leftarrow$ 
      SemanticSearch( $q_i, \mathcal{L}$ )
5:   Extract final pose from previous segment (if available)
6:   Construct prompt  $\mathcal{P}$  including:
7:     - Emotional phrase and text segment
8:     - Retrieved gesture examples  $\{(K_j, V_j)\}$ 
9:     - Physical and stylistic constraints from  $\mathcal{C}$ 
10:    - Transition constraints (final pose continuity)
11:   Generate motion:  $\tilde{g}_i \leftarrow \text{LLMGenerate}(\mathcal{P})$ 
12:   if ConstraintViolation( $\tilde{g}_i, \mathcal{C}$ ) then
13:     Refine prompt with simplified constraints
14:     Re-generate motion:  $\tilde{g}_i \leftarrow \text{LLMGenerate}(\mathcal{P}')$ 
15:   end if
16:   Append to result:  $\mathcal{G} \leftarrow \mathcal{G} \cup \{\tilde{g}_i\}$ 
17: end for

```

---

Conditioned on this prompt, the LLM interprets semantic and biomechanical constraints to synthesize motion segments. The LLM responds with robot-executable keyframe code in a structured format, using precise time-aligned primitives for each joint. Each segment spans a defined duration (e.g., 0.1–1.8s), with timing resolution controlled at the 0.0001s level.

This approach bypasses the need for traditional motion optimization pipelines by embedding constraints and stylistic priors directly into the generation prompt. A complete example of prompt structure and generated keyframe output is provided in Appendix .

#### C. Real-Time Motion Coordination

1) *Temporal Alignment Strategy:* Achieving precise synchronization between speech and gestures is essential for natural interaction. Instead of relying on fixed timing or offline warping techniques, we propose a dynamic alignment strategy that is jointly governed by estimated speech duration and proportional keyframe weighting.

a) *Step 1. Adaptive Duration Estimation:* The total gesture duration  $T$  is modulated based on the predicted speech duration  $\hat{T}$ , adjusted by a smooth scaling factor  $\beta \in [0.9, 1.1]$  that reflects real-time emotional rhythm:

$$T = \beta \cdot \hat{T} \quad (1)$$

b) *Step 2. Time Allocation Across Keyframes:* The duration of each motion segment is governed by learned weights  $\alpha_i$ , which satisfy  $\sum_{i=1}^n \alpha_i = 1$ . The start time  $t_i$  of the  $i$ -th keyframe is calculated as:

$$t_i = T \cdot \sum_{k=1}^{i-1} \alpha_k \quad (2)$$

c) *Step 3. Gesture Trajectory Synthesis:* The complete gesture trajectory,  $G_t$  is composed of motion primitives  $F_i(t; \theta_i)$ , such as Bézier curves or splines, weighted by  $\alpha_i$  and activated over their respective time intervals:

$$G_t = \sum_{i=1}^n \alpha_i \cdot F_i(t; \theta_i) \cdot \mathbb{I}_{[t_i, t_{i+1})}(t) \quad (3)$$

Here,  $\mathbb{I}_{[t_i, t_{i+1})}(t)$  is an indicator function that selects the active time segment, and  $\theta_i$  encodes motion-specific parameters (e.g., joint angles, speed profiles).

2) *Fault-Tolerance Mechanism:* To accommodate the variability inherent in real-world speech, our framework includes a fault-tolerance mechanism to address potential mismatches between expected and actual speech durations. A mismatch is detected when the real-time speech playback deviates from the predicted duration used for gesture alignment. This is monitored by tracking the speech playback timestamp in parallel with scheduled motion keyframes.

$$e_{\text{sync}} = \frac{1}{N} \sum_{i=1}^N |t_i^{\text{speech}} - t_i^{\text{motion}}| \quad (4)$$

where  $t_i^{\text{speech}}$  is the actual timestamp of the speech stream, and  $t_i^{\text{motion}}$  is the expected gesture timing derived from our alignment plan (Section 3.3.1). If  $e_{\text{sync}}$  exceeds a predefined threshold  $\epsilon_{\text{th}}$ , the system enters a degraded mode.

When discrepancies are detected, gesture sequences are adjusted by either motion sequence simplification (see Section 3.3.2) or keyframe resynchronization (as described in Section 3.3.1 Step 2), depending on the severity of the misalignment. This ensures graceful degradation and maintains temporal coherence under real-time constraints.

3) *Constraint-Aware Replanning Strategy:* When LLM-generated gestures violate biomechanical constraints (e.g., joint limits, excessive velocity), the system activates a two-mode recovery strategy:

- **Backtrack Mode:** If a violation occurs in the most recent segment, the system preserves the last valid pose and updates the LLM prompt with failure diagnostics and terminal configuration to generate a locally corrected continuation.
- **From-Scratch Mode:** For persistent failure or degenerative prompts, a complete re-generation is invoked. A fresh set of examples is retrieved, and the LLM is guided to avoid previously observed errors via revised constraints and template adjustments.

The selection between modes depends on violation logs and retry history. These strategies ensure motion robustness across complex or ambiguous utterances. Examples of recovery prompt templates are illustrated in Fig 6 in Appendix, the text highlighted in orange indicate Backtrack updates and blue highlights represent From-Scratch generation.

## IV. EXPERIMENTS

### A. Experimental Setup

a) *Evaluation Setup and System Constraints:* We evaluate our system on the NAO humanoid robot, focusing on

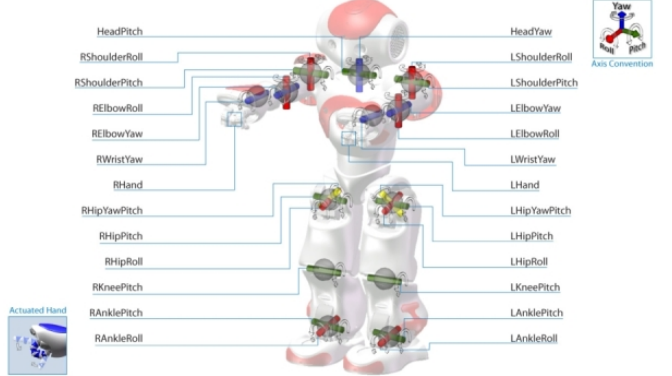


Fig. 3: Overview of NAO’s joint structure.

synchronization accuracy, motion naturalness, and emotional expressiveness. Due to the inherent hardware and control limitations of the NAO platform, several constraints must be addressed in both motion representation and execution. First, the NAO supports only 25 controllable joints (e.g., HeadYaw, LShoulderPitch, etc.), and does not allow continuous mesh outputs or SMPL/SMPL-X style representations. Instead, it requires motion commands to be defined via discrete keyframes, each specifying joint angles at a precise timestamp. This precludes the use of continuous pose streaming or high-frequency trajectory updates.

Furthermore, NAO performs linear interpolation between keyframes without native support for dynamic re-planning or online adaptation, limiting the granularity and flexibility of real-time execution. In addition, due to its limited onboard computational resources, the deployment of heavy neural models such as diffusion-based motion generation is infeasible. To accommodate these challenges, we adopt a lightweight, keyframe-based gesture representation aligned with speech prosody, where each segment is conditioned on semantic content and valence-arousal emotional descriptors.

To analyze the contribution of each component, we implement six model configurations: (1) **PreDefined Gesture Library**, using fixed motions without adaptation; (2) **Speech-Only**, aligned purely with predicted speech timing; (3) **Text-Only**, driven by semantic input without synchronization; (4) **NoSync**, disabling the temporal alignment module; (5) **NoEmotion**, omitting affective scaling; and (6) **ReSIn-HR (Full Model)**, which integrates all modules for emotion-aware, temporally aligned generation.

This setup enables a systematic comparison between static, unimodal, and fully adaptive variants, highlighting the contribution of each module.

### B. Evaluation Metrics

We evaluate our gesture generation system using three metrics that reflect temporal alignment, subjective quality, and emotional consistency.

a) *Temporal Synchronization Accuracy (TSA):* To measure how well generated gestures align with speech, we compute **TSA**, which quantifies the average temporal offset between gesture keyframes and corresponding speech durations. A lower TSA indicates better synchronization. The

formulation is as follows:

$$TSA = \frac{1}{M} \sum_{j=1}^M |t_j^{\text{gesture}} - \lambda_j t_j^{\text{speech}}| \quad (5)$$

Here,  $t_j^{\text{gesture}}$  is the gesture keyframe time,  $t_j^{\text{speech}}$  is the corresponding speech time, and  $\lambda_j$  is a global scaling factor.

b) *Low-Level Motion Smoothness (Jerk)*: To evaluate biomechanical fluidity, we compute the mean angular jerk (i.e., third derivative of angle) across key joints under different emotional conditions. Jerk reflects C2 continuity, and lower values suggest smoother, more expressive motion. We find that the **ReSIn-HR** consistently produces lower jerk across all emotion conditions and joints compared to the **PreDefined** baseline, validating the benefits of emotion-conditioned planning.

c) *User Study Metrics (GA / EC / ON)*: To evaluate the perceptual quality of the generated gestures, we conducted a user study where 20 participants rated the system output using a **7-point Likert scale** along three dimensions: **Gesture Appropriateness (GA)**, which measures how well the gestures match the speech content; **Emotion Compatibility (EC)**, which reflects the extent to which gestures convey the intended emotion; and **Overall Naturalness (ON)**, which assesses the fluidity and realism of the movements.

### C. Quantitative Evaluation

We evaluate system performance using two core metrics: **Temporal Synchronization Accuracy (TSA)** and **Motion Smoothness (Jerk)**.

TABLE I: Temporal Synchronization Accuracy (TSA) and Execution Latency

Model	TSA (ms) $\downarrow$	Latency (ms)
PreDefined	$635 \pm 40$	30
Speech-Only	$168 \pm 18$	47
Text-Only	$492 \pm 30$	46
No Sync	$388 \pm 32$	60
No Emotion	$225 \pm 20$	65
<b>ReSIn-HR</b>	<b><math>218 \pm 23^{**}</math></b>	<b>85 (max: 100)</b>

\*\* Statistically significant ( $p < 0.01$ )

$\downarrow$  indicates lower is better

a) *Temporal Synchronization Accuracy (TSA)*: As shown in Table I, **ReSIn-HR** achieves the best results, with the lowest TSA (218ms), indicating precise speech-motion alignment. While the **Speech-Only** model achieves a slightly lower TSA (168ms), it lacks semantic and emotional grounding. In contrast, the **Text-Only** model captures semantics but performs poorly in temporal alignment (TSA: 492ms).

b) *Motion Smoothness*: we evaluate low-level motion smoothness via mean angular jerk across key joints (e.g., LShoulderPitch, LEbowRoll, HeadPitch). As shown in Fig 4, **ReSIn-HR** consistently achieves lower jerk across emotions (Happy: 1.60, Sad: 1.43, Angry: 1.77) compared to the **PreDefined** baseline, confirming the benefits of emotion-conditioned planning.

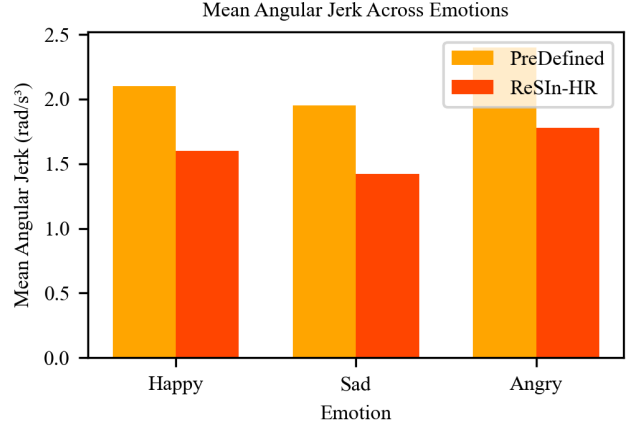


Fig. 4: Mean angular jerk ( $\text{rad/s}^3$ ) across emotions. Lower jerk values indicate smoother, more natural gestures.

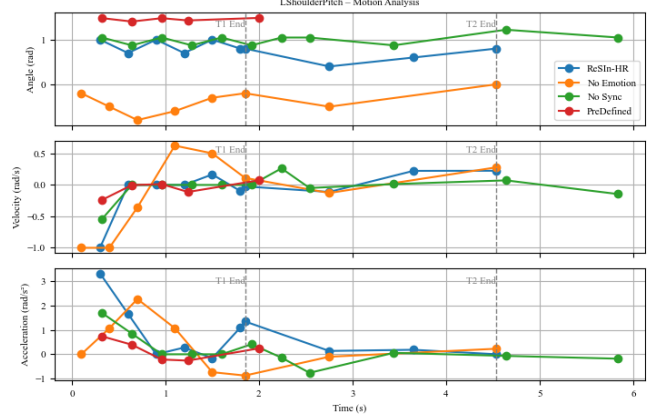


Fig. 5: Joint motion trajectory analysis across models.

c) *Ablation Study*: To assess individual module contributions, we ablate synchronization (**NoSync**) and emotion modulation (**NoEmotion**) respectively. Disabling synchronization increases TSA to 388ms, confirming its importance for timing accuracy. Omitting emotion conditioning leads to higher jerk and reduced emotional expressiveness, emphasizing the role of affect-aware scaling. These results highlight the complementary value of both modules in maintaining coherence and naturalness.

In addition, we report **Execution Latency** to assess run-time feasibility on physical robots (As shown in Table I). **ReSIn-HR** incurs the highest execution latency (average: 85ms), primarily due to real-time gesture modulation and alignment computations. Despite this, the latency remains well within acceptable thresholds for interactive human-robot interaction on the NAO platform. While static gesture libraries enable faster inference, they sacrifice adaptability. Our system balances computational latency with motion naturalness, prioritizing perceptual quality without exceeding platform-specific tolerances.

d) *Visualization Results*: We visualize **LShoulderPitch** trajectories across four models to assess temporal dynamics and biomechanical quality. As shown in Fig 5, **ReSIn-HR** exhibits smooth and expressive motion across both utterance

segments (T1: 0–1.85s, T2: 1.85–4.54s). In the **angle plot**, ReSIn-HR displays broad, emotionally modulated excursions (e.g., peaks near  $t = 1.2$ ,  $t = 2.4$ s), with natural recovery between segments. In contrast, **PreDefined** remains static, while **NoEmotion** shows delayed and compressed movement. **NoSync** produces higher amplitude but lacks temporal alignment, with abrupt changes post  $t = 2.5$ s. In the **velocity** and **acceleration** plots, ReSIn-HR achieves smoother transitions and lower peaks, indicating stable, physically feasible motion. Other variants suffer from sharp spikes or oscillations, especially in **NoSync**, suggesting poor coupling with speech dynamics.

*e) User Study:* A user study with 20 participants evaluated gestures from all six models using a 7-point Likert scale across three criteria: **Gesture Appropriateness (GA)**, **Emotion Compatibility (EC)**, and **Overall Naturalness (ON)**. As shown in Table II, **ReSIn-HR** achieved the highest scores (GA: 4.5, EC: 4.2, ON: 4.6), with statistically significant margins ( $p < 0.01$ ) over all baselines. Participants highlighted its enhanced fluency, emotional alignment, and synchrony. Notably, emotion compatibility improved by 21% over the rule-based **PreDefined** baseline (4.2 vs. 3.4), demonstrating the impact of affect-aware motion scaling on expressive gesture generation.

TABLE II: User Study Ratings on Gesture Quality (Mean  $\pm$  SD)

Model	GA	EC	ON
PreDefined	$3.6 \pm 0.4$	$3.4 \pm 0.5$	$3.7 \pm 0.4$
Speech-Only	$4.1 \pm 0.3$	$3.6 \pm 0.4$	$4.0 \pm 0.3$
Text-Only	$4.2 \pm 0.3$	$3.7 \pm 0.3$	$4.3 \pm 0.3$
No Sync	$4.4 \pm 0.3$	$4.0 \pm 0.4$	$4.5 \pm 0.3$
No Emotion	$4.5 \pm 0.2$	$4.1 \pm 0.3$	$4.6 \pm 0.2$
<b>ReSIn-HR</b>	<b><math>4.5 \pm 0.2^{**}</math></b>	<b><math>4.2 \pm 0.3^{**}</math></b>	<b><math>4.6 \pm 0.2^{**}</math></b>

GA = Gesture Appropriateness, EC = Emotional Congruence, ON = Overall Naturalness.

Scores based on 7-point Likert scale (1 = very poor, 7 = excellent).

\*\* Statistically significant difference ( $p < 0.01$ ).

## V. CONCLUSION

We present ReSIn-HR, a real-time, emotion-aware gesture generation framework for humanoid robots, combining prosody, semantics, and affect into synchronized co-speech motion. Our system features a dual-channel LLM-based architecture, a duration-aware alignment mechanism, and a biomechanical validation loop for safe execution on NAO.

Our experiments demonstrated significant improvements in naturalness, emotional congruence, and synchronization over baseline methods. While the NAO’s hardware limitations restrict the richness of possible motions, future work will explore personalization, latency reduction, and multimodal extensions. This work contributes toward expressive, embodied human-robot interaction, and we plan to release the code and models for community soon.

## REFERENCES

- [1] C. Breazeal, “Toward sociable robots,” *Robotics and autonomous systems*, vol. 42, no. 3-4, pp. 167–175, 2003.
- [2] P. Zhang, P. Liu, H. Kim, P. Garrido, and B. Chaudhuri, “Kinmo: Kinematic-aware human motion understanding and generation,” *arXiv preprint arXiv:2411.15472*, 2024.
- [3] Y. Wu, L. Zhu, Y. Yan, and Y. Yang, “Dual attention matching for audio-visual event localization,” in *Proceedings of the IEEE/CVF international conference on computer vision*, 2019, pp. 6292–6300.
- [4] S. Robotics, “Nao technical specifications,” SoftBank Group Corp., Tech. Rep., 2018. [Online]. Available: <https://www.softbankrobotics.com>
- [5] U. Bhattacharya, E. Childs, N. Rewkowski, and D. Manocha, “Speech2affectivegestures: Synthesizing co-speech gestures with generative adversarial affective expression learning,” in *Proceedings of the 29th ACM International Conference on Multimedia*, 2021, pp. 2027–2036.
- [6] T. Kucherenko, D. Hasegawa, G. E. Henter, N. Kaneko, and H. Kjellström, “Analyzing input and output representations for speech-driven gesture generation,” in *Proceedings of the 19th ACM International Conference on Intelligent Virtual Agents*, 2019, pp. 97–104.
- [7] J. Ho, A. Jain, and P. Abbeel, “Denoising diffusion probabilistic models,” *Advances in neural information processing systems*, vol. 33, pp. 6840–6851, 2020.
- [8] G. Tevet, S. Raab, B. Gordon, Y. Shafir, D. Cohen-Or, and A. H. Bermano, “Human motion diffusion model,” *arXiv preprint arXiv:2209.14916*, 2022.
- [9] J. Chen, Y. Liu, J. Wang, A. Zeng, Y. Li, and Q. Chen, “Diffsheg: A diffusion-based approach for real-time speech-driven holistic 3d expression and gesture generation,” in *Proceedings of the IEEE/CVF Conference on Computer Vision and Pattern Recognition*, 2024, pp. 7352–7361.
- [10] J. Liang, W. Huang, F. Xia, P. Xu, K. Hausman, B. Ichter, P. Florence, and A. Zeng, “Code as policies: Language model programs for embodied control,” in *2023 IEEE International Conference on Robotics and Automation (ICRA)*. IEEE, 2023, pp. 9493–9500.
- [11] A. Brohan, N. Brown, J. Carbajal, Y. Chebotar, X. Chen, K. Chormanski, T. Ding, D. Driess, A. Dubey, C. Finn *et al.*, “Rt-2: Vision-language-action models transfer web knowledge to robotic control,” *arXiv preprint arXiv:2307.15818*, 2023.
- [12] Y. Zhang, D. Huang, B. Liu, S. Tang, Y. Lu, L. Chen, L. Bai, Q. Chu, N. Yu, and W. Ouyang, “Motiongpt: Finetuned llms are general-purpose motion generators,” in *Proceedings of the AAAI Conference on Artificial Intelligence*, vol. 38, no. 7, 2024, pp. 7368–7376.
- [13] S. Marsella, Y. Xu, M. Lhommet, A. Feng, S. Scherer, and A. Shapiro, “Virtual character performance from speech,” in *Proceedings of the 12th ACM SIGGRAPH/Eurographics symposium on computer animation*, 2013, pp. 25–35.
- [14] I. Poggi, C. Pelachaud, F. de Rosis, V. Carofiglio, and B. De Carolis, “Greta: a believable embodied conversational agent,” in *Multimodal intelligent information presentation*. Springer, 2005, pp. 3–25.
- [15] J. Cassell, C. Pelachaud, N. Badler, M. Steedman, B. Achorn, T. Becket, B. Douville, S. Prevost, and M. Stone, “Animated conversation: rule-based generation of facial expression, gesture & spoken intonation for multiple conversational agents,” in *Proceedings of the 21st annual conference on Computer graphics and interactive techniques*, 1994, pp. 413–420.
- [16] I. Habibie, W. Xu, D. Mehta, L. Liu, H.-P. Seidel, G. Pons-Moll, M. Elgharib, and C. Theobalt, “Learning speech-driven 3d conversational gestures from video,” in *Proceedings of the 21st ACM International Conference on Intelligent Virtual Agents*, 2021, pp. 101–108.
- [17] M. Loper, N. Mahmood, J. Romero, G. Pons-Moll, and M. J. Black, “Smpl: A skinned multi-person linear model,” in *Smpl: Seminal Graphics Papers: Pushing the Boundaries, Volume 2*, 2023, pp. 851–866.
- [18] H. Zhang, Y. Tian, Y. Zhang, M. Li, L. An, Z. Sun, and Y. Liu, “Pymaf-x: Towards well-aligned full-body model regression from monocular images,” *IEEE Transactions on Pattern Analysis and Machine Intelligence*, vol. 45, no. 10, pp. 12 287–12 303, 2023.
- [19] G. Pavlakos, V. Choutas, N. Ghorbani, T. Bolkart, A. A. Osman, D. Tzionas, and M. J. Black, “Expressive body capture: 3d hands, face, and body from a single image,” in *Proceedings of the IEEE/CVF conference on computer vision and pattern recognition*, 2019, pp. 10 975–10 985.

- [20] A. Boukhayma, R. d. Bem, and P. H. Torr, “3d hand shape and pose from images in the wild,” in *Proceedings of the IEEE/CVF conference on computer vision and pattern recognition*, 2019, pp. 10 843–10 852.
- [21] X. Qi, J. Pan, P. Li, R. Yuan, X. Chi, M. Li, W. Luo, W. Xue, S. Zhang, Q. Liu *et al.*, “Weakly-supervised emotion transition learning for diverse 3d co-speech gesture generation,” in *Proceedings of the IEEE/CVF Conference on Computer Vision and Pattern Recognition*, 2024, pp. 10 424–10 434.
- [22] T. Kucherenko, P. Jonell, Y. Yoon, P. Wolfert, and G. E. Henter, “The genea challenge 2020: Benchmarking gesture-generation systems on common data,” 2020.
- [23] J. Li, D. Kang, W. Pei, X. Zhe, Y. Zhang, Z. He, and L. Bao, “Audio2gestures: Generating diverse gestures from speech audio with conditional variational autoencoders,” in *Proceedings of the IEEE/CVF International Conference on Computer Vision*, 2021, pp. 11 293–11 302.

## APPENDIX

This appendix illustrates a full pipeline trace of our system generating expressive motion for the NAO robot in response to emotional speech.

### A. Input and Emotion Recognition

- **Audio File:** 03-01-01-01-02-01-01.wav
- **Transcript:** *Kids are talking by the door.*
- **Recognized Emotion:** < | NEUTRAL | >

### B. Generated Emotional Responses

**T1:** *“That sounds like a nice scene.”* (Valence = +7, Arousal = +5) – happy, curious

**T2:** *“Are you curious about what they’re saying?”* (Valence = +6, Arousal = +4) – hopeful, interested

### C. Speech Synthesis Parameters

- **Pitch Modifier:** 1.25
- **Volume Modifier:** 0.75
- **Durations:** 1.51s (T1), 2.13s (T2)

### D. Gesture Planning Description

*Segment 1 (0.1–1.51s):* Moderate amplitude, emotionally expressive upper-body motion with stable lower-body posture.

*Segment 2 (1.51–3.63s):* Outward hand gestures and subtle head turns indicating curiosity and engagement.

#### Listing 1: Segment 1: Head, Arm, Hip Motion

```
names.append("HeadPitch")
times.append([0.3, 0.6, 0.9, 1.2, 1.5062])
keys.append([-0.1, -0.3, -0.1, -0.2, -0.1])
...
```

#### Listing 2: Segment 2: Expressive Gesture

```
names.append("HeadYaw")
times.append([1.5, 1.9, 2.3, 2.7, 3.1, 3.63])
keys.append([0.0, 0.1, -0.1, 0.1, -0.1, 0.0])
...
```

### E. Prompt Recovery Strategy

**System message:** You are an expert humanoid motion planner embedded in a NAO robot. Your task is to generate keyframe-based full-body gestures that are emotionally expressive... Your outputs must:- Respect NAO’s physical constraints (joint limits, max velocity, symmetry).- Avoid abrupt or repetitive motions.- Begin from a specific joint pose (given as feedback). Satisfy both semantic intent and emotional tone. **You are expected to revise a failed plan by:**

(1) Adjusting the joint trajectory or timing...

**Task Description (per input):**  
Generate a motion segment for the phrase: "{text}"Associated emotion:"{query}" (e.g., "I feel so sorry", "I'm excited to meet you")Speech duration:{start\_time} ~ {end\_time} seconds. **Failure context:** The previous generated segment caused: - {reason1} (e.g., "HeadYaw exceeded rotation limit")- {reason2} (optional)Final valid joint pose (as starting point):{pose\_context}

[Optional From Scratch]: No prior pose used. Generate gesture from semantic + emotional query

**Output Format:**{"Reasoning": "The previous plan failed due to over-rotation of LShoulderPitch. I will reduce amplitude and enforce smoother transitions from the given pose.", "GesturePlan": [{"description": "Start with a neutral posture and slow left-arm raise", "joint\_names": ["LShoulderPitch", "LElbowYaw", "HeadPitch"], "keyframes": [{"time": 0.3, "values": [1.0, 1.2, -0.1]}, {"time": 0.6, "values": [0.8, 1.1, -0.2]}, {"time": 0.9, "values": [1.0, 1.2, -0.1]}]}]}

Fig. 6: Prompt templates used in constraint-aware recovery. **Orange = Backtrack, Blue = From Scratch.**

### F. Remarks

- Gesture sequences reflect both semantic content and emotional valence-arousal.
- Each segment is temporally aligned with its speech output.
- Generated joint motions respect NAO’s physical limits.